

Momentum Content of Single-Nucleon Halos

P. G. Hansen

*National Superconducting Cyclotron Laboratory and Department of Physics and Astronomy,
Michigan State University, East Lansing, Michigan 48824-1321*

(Received 12 January 1996)

The longitudinal momentum distributions of the core fragment in the dissociation of halo states on light targets provide information pertaining to the external part of the halo. The calculations agree well with the measured momentum widths and cross sections for the reactions (^{11}Be , ^{10}Be) and (^8B , ^7Be). The measured widths are not expected to be sensitive to the instrumental transverse-momentum acceptance. [S0031-9007(96)00770-3]

PACS numbers: 21.10.Gv, 25.60.Ge, 25.70.Mn, 27.20.+n

Nuclear halos [1] are characterized by the low binding of the last nucleon (or pair) and by having an appreciable single-particle component of low angular momentum. Their wave functions can best be studied in momentum coordinates, where the wide spatial distributions translates into a narrow momentum distribution. This connection was first explored by Serber [2] for the deuteron, the mother of all halo states, and for reactions at high energy (95 MeV/u), at which the interaction with a light target is essentially instantaneous. The neutron and the proton spend most of the time outside the range of their interaction, and the removal of one of them will leave the other with the momentum it had at the instant of the collision. Serber referred to this process as “stripping,” an obscure reference to a procedure in weapons technology, see his recent remarks on the subject [2]. Modern work on halo states frequently invokes the Serber mechanism to justify the assumption that the momentum distribution of a fragmentation product will be that of the initial wave function. In the following it will be shown that this does not hold in general. The essential point, recently noted by several authors [3–5], is that a halo state differs from the dumb-bell structure of the deuteron, and that collisions with a nuclear target cannot explore all parts of the halo’s spatial wave function with equal probability. As a consequence, the observed momentum distributions relate to the outer part of the halo structure and are, in fact, more specific and more interesting than had been thought initially.

The momentum components transverse to the beam direction are known from experiment [1] to carry the imprint of the reaction mechanism. For the parallel momentum components, experiments [6] suggested, as we shall see correctly, that the mechanism would play a smaller role. Theory [7–9] subsequently argued that the parallel distribution would, indeed, be close to that of the total halo state, one argument being that the nuclear interactions will not lead to localization of the wave function along the beam direction. It will be seen from what follows that this is true for wave functions that factorize in cylindrical coordinates such as plane waves and Gaussians. However, the external two-body wave

functions appropriate for halo states do not factorize, and the effect to be discussed arises from localization perpendicular to the beam direction.

The analysis can be simplified in a number of ways. Except for a brief remark about Coulomb dissociation towards the end, it is here restricted to purely nuclear reactions of single-nucleon halo systems with light targets. Good data exist for ^{11}Be [10] and ^8B [11,12], for which the structure is well understood [3,13,14] as predominantly an s -state halo neutron and a p -state halo proton, respectively. It is a good first approximation to represent these by a single-particle product wave function ψ_0 . The high projectile energies allow a description in terms of a classical impact parameter b , see Fig. 1. The dissociation products ^{10}Be or ^7Be are formed at impact parameters greater than $b_{\min} = R_C + R_A$, where the energy-dependent core and target radii are chosen to reproduce measured heavy-ion interaction cross sections [15]. There are two reaction channels: (i) nucleon stripping (or absorption) in which the halo nucleon has interacted strongly with the target and disappears from the beam, and (ii) diffraction dissociation in which the nucleon moves forward with essentially beam velocity. Collisions at impact parameters smaller than b_{\min}

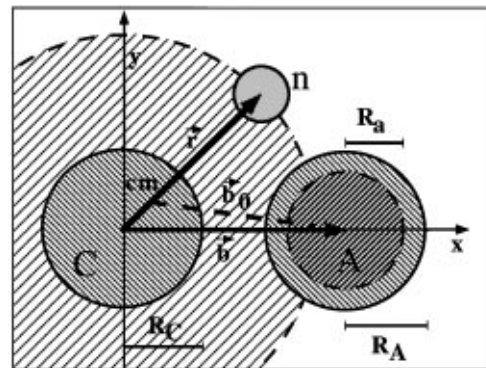


FIG. 1. The coordinate system is centered in the projectile core C relative to which coordinate of the halo neutron is r . The impact parameter of the target A (moving along the z axis) is approximated by the two-dimensional vector b instead of the vector b_0 connecting to the center of mass. The target radii are the heavy-ion interaction radius R_A and the nucleon interaction radius R_C .

are assumed to lead to core fragmentation and hence will not contribute to the dissociation cross section.

The high beam energy also implies that the eikonal approximation is applicable. The target trajectory (in the coordinate system used here) is a straight line, and the range of the interaction, which does not have to be weak, is of the order of the effective target radius R_a . In this approximation, see Gottfried [16], the wave function of the halo state ψ_0 remains unchanged throughout all space except in a cylinder of radius R_a , where it is set to zero. This is the commonly used black-disk model. Its most important limitation, the assumption of a sharp target surface, is of little consequence in a discussion of the longitudinal momentum components. Let the wave function originally contained in the reaction zone be denoted $\delta\psi_0$, a function that vanishes outside the interaction radius R_a , which can be chosen to reproduce the experimental reaction and elastic cross sections for free nucleons.

Finally, the sudden approximation is valid. At the moment of impact, the nucleon stripping reaction selects the state of the system to be $\delta\psi_0$. The normalization P_a of this state is the stripping probability for a given b , and the square of its three-dimensional Fourier transform gives the momentum distribution, which must be that of the core fragment since the halo nucleon is no longer present. For the same reason, the question of final-state interactions does not arise. If the nucleon is not stripped, the new state represented by the complement of the wave function $\psi_0 - \delta\psi_0$ is mainly the unchanged halo state. The (small) probability that it decays by diffraction dissociation is obtained directly if it is assumed [17] that the halo state ψ_0 is the only bound state of the system, which can be projected out to give the wave function of the decaying state $\psi_d = P_a\psi_0 - \delta\psi_0$ with normalization of $P_a - P_a^2$. It will be seen that the first term in the wave function of the decaying state is a small correction, necessary to preserve orthogonality. Hence the probabilities of stripping and diffraction dissociation are approximately identical and equal to P_a . (This is related to the fact that the total cross section for fast neutrons is approximately twice the geometrical value.) If final-state interactions are neglected, which seems to be a good approximation for ^{11}Be [17], the momentum distribution for diffraction dissociation is also given by the square of the Fourier transform of $\delta\psi_0$, which is than all that needs to be calculated.

To obtain the probability distribution in momentum (written in terms of the wave vector \mathbf{k}) along the z axis for a general wave function $\psi(\mathbf{r})$, the square of its Fourier transform is integrated over k_x and k_y . This fivefold integral can be reduced to

$$\frac{dW}{dk_z} = \frac{1}{2\pi} \int \int \int \int \psi^*(x, y, z') \psi(x, y, z) \times \exp[ik_z(z - z')] dx dy dz dz', \quad (1)$$

a quantity that must now be evaluated with the wave function $\delta\psi_0$ introduced above. The differential cross section

$$\frac{d\sigma}{dk} = \int_{b_{\min}}^{\infty} \frac{dW}{dk_z} d\varphi b db \quad (2)$$

emerges as an integral over impact parameter.

For a narrow reaction zone with radius R_a it is a good approximation to replace the wave function in the integrand in (1) by its value $\psi_0(b, 0, z)$ along the target trajectory. The integral over x and y now gives a factor πR_a^2 , which may be interpreted as the (free) nucleon reaction cross section. The contribution from diffraction dissociation relates in the same way to the elastic nucleon-target cross section. The sum of the two is obtained by replacing $2\pi R_a^2$ with the experimental [18] total cross section σ_T . If the integrand is symmetric about the z axis, Eq. (1) can be approximated as

$$\frac{dW}{dk_z} \approx \frac{\sigma_T}{2\pi} \left| \int \exp(-ik_z z) \psi_0(b, 0, z) dz \right|^2 \quad (3)$$

since the two integrals over z and z' factorize. For initial states with l equal to 1 or greater, this expression must be averaged over initial m states in the usual way. It can easily be shown that, when taken in the limit of b_{\min} equal to zero, the integrals (3) followed by (2) give the true momentum distribution of the complete wave function, obtained more directly by substituting ψ_0 into Eq. (1).

For the case of a halo neutron with $l = 0, 1$, it is easy to derive closed expressions for Eqs. (2) and (3). As the reaction zone $\delta\psi_0$ is entirely outside the nuclear core, the exact external wave function is the first spherical Hankel function

$$\psi_0(r) = B\kappa^{3/2} h_l(i\kappa r) Y_{lm}(\vartheta, \varphi) \quad (4)$$

written in terms of the reduced mass and neutron separation energy through the relation $\kappa = (2\mu S_n)^{1/2}/\hbar$. The dimensionless constant B , of order unity, is determined by joining the outer and inner solutions to the Schrödinger equation. For an $l = 0$ state, a Yukawa wave function corresponds to the choice $B = \sqrt{2}$ (sometimes [17] augmented by a finite-size correction), while a Woods-Saxon calculation suggests $B = 2.26$ for ^{11}Be . For a p state and a neutron binding energy of 0.137 MeV (corresponding to that of the proton in ^8B), one has $B = 0.47$.

The integral (3) for $l = 0$ is given in Sect. 3.961 of [19],

$$\frac{dW_0}{dk_z} = \frac{\sigma_T B^2 \kappa}{2\pi^2} K_0^2(\chi), \quad (5)$$

and partial differentiation of the two integrals given in the same reference with respect to the impact parameter b leads to the expression for $l = 1$,

$$\frac{dW_l}{dk_z} = \frac{\sigma_T B^2}{2\pi^2 \kappa} [k_z^2 K_0^2(\chi) + (k_z^2 + \kappa^2) K_1^2(\chi)], \quad (6)$$

where the argument of the modified Bessel functions is $\chi = b(\kappa^2 + k_z^2)^{1/2}$. The two terms inside the square bracket in Eq. (6) are the contributions from the $m = 0$ and $m = \pm 1$, respectively, the latter being the most important. The differential cross sections can now be obtained by integrating Eqs. (5) and (6) over b to give for $l = 0$

$$\frac{d\sigma_0}{dk_z} = \frac{\sigma_T B^2 \kappa b_{\min}^2}{2\pi} [K_1^2 - K_0^2] \quad (7)$$

and for $l = 1$

$$\frac{d\sigma_1}{dk_z} = \frac{\sigma_T B^2 b_{\min}^2}{2\pi \kappa} \left[k_z^2 (K_1^2 - K_0^2) + (k_z^2 + \kappa^2) \times \left(K_2^2 - K_1^2 - \frac{2}{\xi} K_1 K_2 \right) \right], \quad (8)$$

where the argument of the modified Bessel functions is understood to be $\xi = b_{\min}(\kappa^2 + k_z^2)^{1/2}$. The single-nucleon stripping cross sections are obtained by integrating over k_z . Results obtained with Eqs. (5)–(8) are shown in Figs. 2 and 3 and in Table I.

Complete single-particle wave functions were calculated in a Woods-Saxon potential-well model with radius and diffuseness parameters $r_0 = 1.25$ fm and $a = 0.7$ fm and with the well depth adjusted to reproduce the experimental separation energy. The results obtained for neutrons when Eqs. (2) and (3) were evaluated numerically with these wave functions were identical with the results of Eqs. (5)–(8) to within 1% as could be expected since, in this case, Eq. (4) is an exact solution outside the range of the potential. For the ${}^8\text{B}$ calculations, Fig. 3 and Table I, the Coulomb potential acting on the halo proton was taken as that of a uniformly charged sphere with the same

radius as the Woods-Saxon well. The results are insensitive to the choice of the Coulomb radius.

The approximation leading to Eq. (3) assumes that the effective radius R_a of the target is small. (At 63 MeV/u it is of the order of 2.0 fm for ${}^9\text{Be}$ as compared with a decay length of the ${}^{11}\text{Be}$ halo wave function of 6.75 fm.) This assumption can be tested in the other extreme limit, that of infinite target radius, in which the reaction zone is bounded by a planar cutoff. Expressions for this case have been given elsewhere [1,4]. The four pairs of dashed curves shown in Fig. 2 demonstrate that the two extreme approximations give nearly identical results, and also that the parallel-momentum distributions depend strongly on the impact parameter.

The momentum distributions of the cross section are shown as large dots in Figs. 2 and 3, and the widths and dissociation cross sections are summarized in Table I, which shows that there is very good agreement with the experimental results [10,11,17,20]. The cross sections, roughly one-third and one-tenth of the free-nucleon values, provide a valuable quantitative verification of the simple model used. It is seen that the calculation, in agreement with that of Esbensen [5], satisfactorily explains the reduction of ${}^8\text{B}$ width to roughly half of that of the total wave function, 153 MeV/c. This apparent discrepancy had originally led to the claim [11] that an interpretation in terms of a complex many-particle wave function was required. As the effect of localization must in any case be present, it should not be viewed as a possible alternative explanation. Two curves in Fig. 3 and the last line in Table I demonstrate that a p -state neutron would behave similarly.

The interpretation given here has an important implication for the analysis of experimental data. Con-

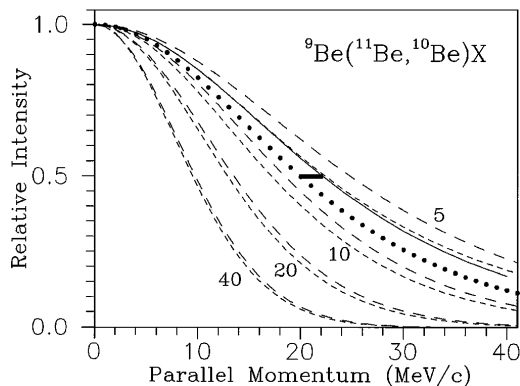


FIG. 2. Calculations for the ${}^{11}\text{Be}$ s -state halo incident on a beryllium target and for a beam energy of 63 MeV/u. (i) All parallel momentum distributions are normalized to unity at the origin; the bar is the measured half width at half maximum, and the large dots represent the differential cross section $d\sigma/dp_z$. The full-drawn line is the distribution dW/dp_z of the total wave function. (ii) The four pairs of dashed curves correspond to the quantity dW/dp_z for fixed impact parameters of 5, 10, 20, and 40 fm with the long and short dashes denoting the respective limits of small target radius [Eq. (5)] and infinite target radius (planar cutoff).

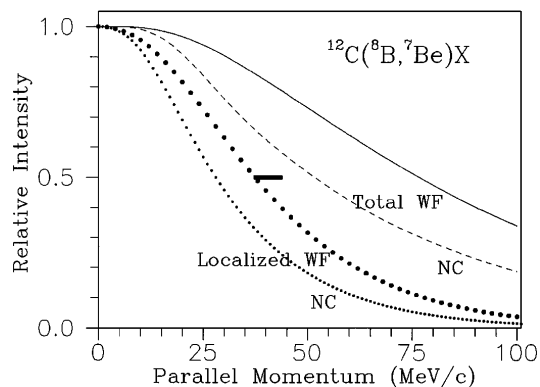


FIG. 3. Calculations for the ${}^8\text{B}$ p -state halo incident on a carbon target and for a beam energy of 1471 MeV/u. The notation is the same as for Fig. 2 (i). It is seen that the localization effect reduces the width by a factor of 2, in agreement with experiment. The other pair of curves, dashed and small dots, are calculated for no Coulomb (NC) interaction in the halo state. The localization effect is, in this case, given by Eq. (8) and illustrates the case of a hypothetical p -state neutron with otherwise unchanged parameters.

TABLE I. Beam energy, widths, and cross sections.

E_B (MeV/u)	FWHM Γ (MeV/c)		free	Cross sections (mb)	
	calc.	exp.		calc.	exp.
(i) Reaction ${}^9\text{Be}({}^{11}\text{Be}, {}^{10}\text{Be})$, $1s$ state, $S_n = 0.504$ MeV, $\Gamma_{\text{tot}} = 44$ MeV/c					
41	39	...	930	316	290 ± 40^a
63	40	42 ± 2^b	690	255	...
460	41	...	235	98	...
(ii) Reaction ${}^{12}\text{C}({}^8\text{B}, {}^7\text{Be})$, $0p$ state, $S_p = 0.137$ MeV, $\Gamma_{\text{tot}} = 153$ MeV/c					
40	69	...	1078	111	80 ± 15^c
1471	75	81 ± 6^d	377	54	94 ± 4^d
1471 ^e	56	...	377	82	...

^aRef. [17], ^bRef. [10], ^cRef. [20], ^dRef. [11], and ^eCalculation with the p - ${}^7\text{Be}$ Coulomb interaction neglected. In this case, $\Gamma_{\text{tot}} = 103$ MeV/c.

trary to what is often assumed [10,21], the longitudinal momentum distributions measured with a light target should, to lowest order, not be affected by the transverse acceptance of the spectrometer. In the approximation leading to Eq. (3) the radial momentum distribution becomes proportional to $[J_1(k_r R_a)/k_r R_a]^2$, the usual diffraction pattern, depending only on the radius of the target. Clearly, all information about the original momentum in the x - y plane has been destroyed by the measurement. The corresponding radial broadening has been detected [1,17] for neutrons. This means that the wave function at the moment of the collision takes a form that factorizes, see earlier comments, and the k_z distribution will not be changed by an incomplete detection of the k_x and k_y components.

Finally, a brief remark about reactions with heavy targets, dominated by Coulomb excitation to the continuum. The fact that these gave [6,10,11] almost the same longitudinal distributions as the light targets was, for a while, taken to suggest that both reflected a common property: the momentum distribution of the initial halo state. This now appears to be a numerical coincidence, and calculations of Coulomb excitation [4,12,17] account satisfactorily for the experimental results. The narrow parallel and broad transverse components seen for the case of ${}^{11}\text{Be}$ arise [4] from the dominant $\sin^2 \vartheta$ term in the angular distribution.

To sum up, this paper has considered the longitudinal momentum distributions in the dissociation reactions (${}^{11}\text{Be}, {}^{10}\text{Be}$) and (${}^8\text{B}, {}^7\text{Be}$) on light targets and gives analytical expressions applicable to neutron halos. No adjustable parameters have been introduced: The absolute differential cross sections are linked directly to measured quantities, primarily the nucleon separation energy and the nucleon and heavy-ion total cross sections.

The author is indebted to Sam M. Austin, Walter Benenson, B. Alex Brown, and Brad M. Sherrill for discussions. Work supported by the National Science Foundation under Grant No. PHY-95-28844.

- [1] P. G. Hansen, A. S. Jensen, and B. Jonson, *Annu. Rev. Nucl. Part. Sci.* **45**, 591 (1995).
- [2] R. Serber, *Phys. Rev.* **72**, 1008 (1947); *Annu. Rev. Nucl. Part. Sci.* **44**, 1 (1994).
- [3] B. A. Brown, A. Csótó, and R. Sherr, *Nucl. Phys.* **A597**, 66 (1996).
- [4] P. G. Hansen, in *Proceedings of the International Conference on Exotic Nuclei and Atomic Masses—ENAM 95, Arles, June 1995*, edited by M. de Saint Simon and O. Sorlin (Editions Frontieres, France, 1995), p. 175.
- [5] H. Esbensen, *Phys. Rev. C* **53**, 2007 (1996).
- [6] N. A. Orr *et al.*, *Phys. Rev. Lett.* **69**, 2050 (1992); *Phys. Rev. C* **51**, 3116 (1995).
- [7] C. A. Bertulani and K. W. McVoy, *Phys. Rev. C* **46**, 2638 (1992).
- [8] H. Sagawa and N. Takigawa, *Phys. Rev. C* **50**, 985 (1994).
- [9] F. Barranco, E. Vigezzi, and R. A. Broglia, Report No. NTGMI-95-2 (to be published).
- [10] J. H. Kelley *et al.*, *Phys. Rev. Lett.* **74**, 30 (1995).
- [11] W. Schwab *et al.*, *Z. Phys. A* **350**, 283 (1995).
- [12] Sam M. Austin *et al.* (to be published).
- [13] H. Sagawa, B. A. Brown, and H. Esbensen, *Phys. Lett. B* **309**, 1 (1993); T. Otsuka, N. Fukunishi, and H. Sagawa, *Phys. Rev. Lett.* **70**, 1385 (1993).
- [14] A. Csótó, *Phys. Lett. B* **315**, 24 (1993).
- [15] I. Tanihata, *Prog. Part. Nucl. Phys.* **35**, 505 (1995).
- [16] K. Gottfried, *Quantum Mechanics* (Benjamin, New York, 1966), Vol. I, p. 114.
- [17] R. Anne *et al.*, *Nucl. Phys.* **A575**, 125 (1994); *Phys. Lett. B* **304**, 55 (1993).
- [18] R. W. Finlay *et al.*, *Phys. Rev. C* **47**, 237 (1993); W. Schimmerling *et al.*, *Phys. Rev. C* **7**, 248 (1973); J. Franz *et al.*, *Nucl. Phys.* **A490**, 667 (1988); G. J. Igo *et al.*, *Nucl. Phys.* **B3**, 181 (1967).
- [19] I. S. Gradshteyn and M. Ryzhik, *Tables of Integrals, Series and Products* (Academic Press, New York, 1965), 4th ed., p. 498.
- [20] I. Pecina *et al.*, *Phys. Rev. C* **52**, 191 (1995).
- [21] K. Riisager, in *Proceedings of the 3rd International Conference on Radioactive Nuclear Beams, East Lansing, Michigan*, edited by D. J. Morrissey (Editions Frontieres, Gif-sur-Yvette, France, 1993), p. 281.